Citation: CPT Pharmacometrics Syst. Pharmacol. (2014) 3, e144; doi:10.1038/psp.2014.42

www.nature.com/psp

ORIGINAL ARTICLE

Population Pharmacokinetics of Obinutuzumab (GA101) in Chronic Lymphocytic Leukemia (CLL) and Non-Hodgkin's Lymphoma and Exposure–Response in CLL

E Gibiansky[1], L Gibiansky[1], DJ Carlile[2], C Jamois[3], V Buchheit[3] and N Frey[3]

Treatment regimens involving obinutuzumab (GA101) demonstrated increased efficacy to rituximab in clinical trials for non-Hodgkin's lymphoma (NHL) and chronic lymphocytic leukemia (CLL). However, the pharmacokinetic (PK) properties and the exposure–response relationships of obinutuzumab still need to be fully described. Data from four clinical trials of obinutuzumab were analyzed to describe the PK properties in patients with NHL or CLL and the pharmacodynamic (PD) properties in patients with CLL. A population PK model with linear time-dependent clearance described the obinutuzumab concentration–time course. Diagnosis, baseline tumor size (BSIZ), body weight, and gender were the main covariates affecting obinutuzumab exposure. In patients with CLL, exposure was not associated with safety but showed positive trends of correlation with efficacy. Although efficacy correlated positively with exposure, since both efficacy and exposure correlated negatively with BSIZ, it was not possible to determine with certainty whether it would be beneficial to adjust the dose according to BSIZ.
CPT Pharmacometrics Syst. Pharmacol. (2014) **3**, e144; doi:10.1038/psp.2014.42; published online 29 October 2014

Treatment regimens containing the anti-CD20 monoclonal antibody rituximab (MabThera; Rituxan, F. Hoffmann-La Roche) have improved clinical outcomes, including survival, in non-Hodgkin's lymphoma (NHL)[1–10] and chronic lymphocytic leukemia (CLL) patients.[4,5,7–11] Consequently, rituximab has become the standard-of-care treatment for these malignancies.[12,13] However, some patients do not respond adequately to rituximab and others eventually relapse. Therefore, there remains an unmet medical need for treatments with improved antitumor activity without increased toxicity.

Obinutuzumab (GA101; Gazyva, F. Hoffmann-La Roche) is a novel, humanized anti-CD20 monoclonal antibody. Obinutuzumab has a glycoengineered Fc region, which facilitates induction of enhanced antibody-dependent cell-mediated cytotoxicity relative to rituximab.[14,15] Obinutuzumab is a type II monoclonal antibody, which increases levels of direct cell death compared with a type I monoclonal antibody such as rituximab.[16–18]

The safety and efficacy of obinutuzumab for the treatment of various CD20+ B-cell malignancies were assessed in four clinical trials. The phase I/II studies GAUSS and GAUGUIN evaluated a wide range of obinutuzumab doses (50–2,000 mg) in patients with CLL, B-cell lymphoma (BCL), diffuse large BCL (DLBCL), mantle cell lymphoma (MCL), or follicular lymphoma.[19–23] In the phase Ib GAUDI study in relapsed/refractory NHL patients, obinutuzumab doses of 400–1,600 mg were assessed,[24] and in the phase III CLL11 study, previously untreated comorbid CLL patients received obinutuzumab 1,000 mg.[25] GAUSS, GAUGUIN, and GAUDI assessed the pharmacokinetics (PK) of obinutuzumab,[20–24] but the relationship of PK to pharmacodynamics (PD) was not evaluated. Here, we report the results of a population PK model for obinutuzumab that integrates data from GAUSS, GAUGUIN, GAUDI and CLL11, and the results of an exploratory graphical exposure–response analysis of obinutuzumab using data from CLL11. The aims of this work were to (i) describe the PK properties of obinutuzumab in CLL and NHL patients, (ii) identify covariates that influence exposure in CLL and NHL patients, and (iii) explore the relationships between exposure and safety, efficacy and PD parameters in CLL patients.

RESULTS

Analysis population

The dataset for the analysis comprised 12,634 quantifiable serum samples from 678 patients treated with obinutuzumab (**Table 1**); 3,446 samples were contributed from GAUGUIN (131 patients; 30 CLL, 101 NHL), 3,634 from GAUDI (134 NHL patients), 2,327 from GAUSS (105 patients; 101 NHL, 4 CLL), and 3,227 from CLL11 (308 CLL patients).

Summary statistics for the covariates in each study and the total analysis population are shown in **Table 2**. In the analysis population, 57.1% were male, mean (range) age was 65.7 years (22–89 years), mean (range) weight was 75.6 kg (40–140 kg), and mean (± standard deviation (SD)) baseline tumor size (BSIZ) was 5,390 (±19,100) mm^2. Patients in CLL11 (comprising previously untreated CLL patients) were older than those in GAUGUIN, GAUDI, or GAUSS, reflecting the inclusion criteria and patient population for CLL11. Additionally, patients in CLL11 had higher B-cell counts at baseline than those in any of the other studies (**Table 2**). Approximately half (342/678) of all patients in this analysis

[1]QuantPharm LLC, North Potomac, Maryland, USA; [2]Roche Products Ltd, Welwyn Garden City, UK; [3]F. Hoffmann-La Roche Ltd, Basel, Switzerland. Correspondence: E Gibiansky (egibiansky@quantpharm.com)
Received 15 May 2014; accepted 6 August 2014; published online 29 October 2014. doi:10.1038/psp.2014.42

Table 1 Summary of studies of obinutuzumab included in the PK analysis

Study	Dosing regimens	PK measurements
GAUGUIN, phase I/II (BO20999; NCT00517530); ITT population: 134; population PK analysis: 3,446 samples from 131 patients	NHL indication 400 mg on days 1 and 8 of cycle 1 and day 1 of cycles 2–8 1,600 mg on days 1 and 8 of cycle 1 and 800 mg on day 1 of cycles 2–8 CLL indication 1,000 mg on days 1, 8, and 15 of cycle 1 and day 1 of cycles 2–8. Patients with disease progression receiving obinutuzumab 400 mg could cross over to 800 mg	Cycle 1 Day 1 predose, immediately after end of infusion and 3–6 h postdose; days 2, 4, 8, 10–11, and 14–21 Cycles 2–7 Day 1 predose and immediately after end of infusion Cycle 8 Day 1 predose, immediately after end of infusion, 3–6 h postdose; days 2, 4, 14–16, and 19–25 Follow-up 28-day safety follow-up (day 176)
GAUDI, phase Ib (BO21000; NCT00825149); ITT population: 136; population PK analysis: 3,634 samples from 134 patients	Relapsed/refractory FL indication FC or CHOP plus either obinutuzumab 400 mg (all administrations) (CHOP arm: on day 1 of 21-day cycles for 6–8 cycles, FC arm: on day 1 of 28-day cycles for 4–6 cycles), or 1,600 mg on days 1 and 8, with 800 mg subsequently. Patients with disease progression receiving obinutuzumab 400 mg could cross over to 800 mg First-line FL indication 1,000 mg obinutuzumab, either every 21 days for 6–8 cycles (CHOP arm) or every 28 days for 4–6 cycles (bendamustine arm) Patients demonstrating a complete or partial response were eligible to receive obinutuzumab as maintenance therapy starting 12 weeks after the last dose	Cycle 1 Day 1 predose, immediately after end of infusion, and 3–6 h postdose; days 2, 4, 8, 10–11, and 14–21 Cycles 2–7 (CHOP) or cycles 2–5 (FC) Day 1 predose and immediately after end of infusion Final cycle Day 1 predose, immediately after end of infusion, 3–6 h postdose; days 2, 4, 14–16, and 19–25 Follow-up 28-day safety follow-up (day 176); every 3 months from last infusion, for 2 years or until B-cell recovery was achieved and at each tumor assessment visit for those patients who were eligible for obinutuzumab maintenance therapy
GAUSS, phase I/II (BO21003; NCT00576758); ITT population: 175; population PK analysis: 2,327 samples from 105 patients	Phase I Multicohort, three-by-three dose-escalation study in patients with $CD20^+$ malignant disease (17 NHL and 5 CLL patients) Cohorts 1–5 (each $n = 3$) and Cohort 6 ($n = 6$) received obinutuzumab at 200, 400, 800, 1,200, 2,000, and 1,000 mg, respectively, during induction therapy (i.e., 4 weekly infusions) Cohort 6 (1,000 mg) was included to provide safety and tolerability data before exploring in phase II Patients who demonstrated a CR/CRu/PR at the end of induction were eligible for entry into a 2-year extended treatment period where they received obinutuzumab once every 3 months	Phase I Cycle 1 Day 1 predose, immediately after end of infusion and 3–6 h postdose; days 2 and 4 Cycles 2–3 Day 1 predose and immediately after end of infusion Cycle 4 Day 1 predose, immediately after end of infusion, 3–6 h postdose; days 2 and 4; 6–8, 12–16, 18–24, and 28–56 days postinfusion Follow-up/maintenance Every 3 months (from last infusion), pre- and post- each infusion and at each tumor assessment visit for patients eligible for 2-year obinutuzumab maintenance therapy. For patients not eligible for obinutuzumab maintenance therapy, a single sample every 3 months for 2 years, or until B-cell recovery was achieved If a patient discontinued the study before cycle 4, the PK sampling schedule for cycle 4 was applied at discontinuation if possible
	Phase II 175 patients randomly received 4 weekly infusions of either obinutuzumab (1,000 mg) or rituximab (375 mg/m^2) as monotherapy An exploratory, nonrandomized third arm ($n = 15$) investigated a shorter duration of obinutuzumab infusion (for infusions 2–4)	Phase II Cycles 1–3 Day 1 predose, immediately after end of infusion Cycle 4 Day 1 predose, immediately after end of infusion; 6–8, 12–16, 18–24, and 28–84 days postinfusion Follow-up/maintenance A single PK sample every 3 months for 2 years or until B-cell recovery was achieved If a patient discontinued the study before cycle 4, the PK sampling schedule for cycle 4 was applied at discontinuation if possible

Table 1 Continued on next page

Table 1 Continued

Study	Dosing regimens	PK measurements
CLL11, phase III (BO21004; CT01010061); ITT population: 238; population PK analysis: 3,227 samples from 308 patients[a]	Stage 1 Comparison of GClb vs. Clb (Stage 1a) and RClb vs. Clb (Stage 1b) Treatment was given for a maximum of 6 cycles of 28 days' duration. In the GClb arm, obinutuzumab was administered as 1,000 mg on days 1, 8, and 15 of cycle 1, and on day 1 of cycles 2–6 Stage 2 Ongoing	Predose and post day 1 infusion of cycles 1–6 Additional PK sampling (30 patients): Cycle 1: days 8 and 15 pre- and postinfusion Follow-up: day 28, and 3, 6, 9, and 12 months after last treatment dose A sample was taken at the last visit for patients who withdrew

CHOP, cyclophosphamide, doxorubicin, vincristine, and prednisone; Clb, chlorambucil; CLL, chronic lymphocytic leukemia; CR, complete response; CRu, complete response unconfirmed; FC, fludarabine and cyclophosphamide; FL, follicular lymphoma; GClb, obinutuzumab and chlorambucil; ITT, intent to treat; NHL, non-Hodgkin's lymphoma; PK, pharmacokinetic; PR, partial response; RClb, rituximab and chlorambucil.
[a]Twenty-three patients had no PK samples. One patient was removed due to inconsistent PK data, and six patients from the open label run-in period were added.

Table 2 Summary statistics of covariates

				Study			
Covariate	Description	Units	Overall	GAUGUIN (BO20999)	GAUDI (BO21000)	GAUSS (BO21003)	CLL11 (BO21004)
N	Number of patients	*n*	678	131	134	105	308
Sex	Male	*n* (%)	387 (57.1)	79 (60.3)	63 (47.0)	57 (54.3)	188 (61.0)
BW	Weight	kg, mean (SD)	75.6 (15.1)	76.1 (15.1)	78.3 (16.7)	77.0 (15.5)	73.7 (14.1)
Age	Age	years, mean (SD)	65.7 (11.7)	63.1 (12.2)	57.1 (11.2)	61.8 (9.8)	71.9 (8.64)
BBCE	Baseline B-cell count	10^9/l, mean (SD)	37.4 (66.6)	11.8 (26.8)	1.62 (10.9)	2.43 (12.6)	77.75 (81.6)
BSIZ	Baseline tumor load	mm^2, mean (SD)	5,390 (19,100)	4,480 (4,470)	5,560 (5,130)	4,420 (5,740)	6,030 (27,780)
CLL	Chronic lymphocytic leukemia	*n* (%)	342 (50.4)	30 (22.9)	—	4 (3.8)	308 (100.0)
BCL	B-cell lymphoma	*n* (%)	286 (42.2)	56 (42.7)	134 (100.0)	96 (91.4)	—
DLBCL	Diffuse large B-cell lymphoma	*n* (%)	30 (4.4)	26 (19.8)	—	4 (3.8)	—
MCL	Mantle cell lymphoma	*n* (%)	20 (2.9)	19 (14.5)	—	1 (1.0)	—

BBCE, baseline B-cell count; BCL, B-cell lymphoma; BSIZ, baseline tumor size; BW, body weight; CLL, chronic lymphocytic leukemia; DLBCL, diffuse large B-cell lymphoma; MCL, mantle cell lymphoma; SD, standard deviation.

had a CLL diagnosis, while the remaining 50% (336/678) had various types of NHL (BCL, DLBCL, or MCL; **Table 2**).

Base PK model development

The model with parallel linear and Michaelis–Menten elimination (MM model) and the model with time-dependent clearance both reduced the objective function (OFV) compared with a linear two-compartment model. However, the decrease in OFV was greater for the model with time-dependent clearance than for the MM model (2,192 vs. 1,149 points). Additionally, the high value of the Michaelis–Menten constant (K_M = 229 µg/ml) in the MM model was inconsistent with target-mediated elimination. Therefore, the model with time-dependent clearance was retained, where clearance was a sum of time-dependent clearance (CL_T) with associated decay coefficient (k_{des}), and time-independent clearance (CL_{inf}). The model was further improved by the introduction of allometric scaling with fixed power coefficients on clearances and volumes of 0.75 and 1, respectively, and by the addition of inter-individual random effect on the proportional residual error.

Covariate model development

As the preliminary investigation indicated that the parameters of the peripheral compartment (intercompartmental clearance (Q) and peripheral volume (V_2)) could not support the covariate effects, the full covariate model included the covariate effects only for the parameters of the central compartment.

In the base model, patients with a low BSIZ (below ~1,500–2,000 mm^2) appeared to have higher k_{des} values than those with a higher BSIZ. Preliminary investigation of dependence of k_{des} on BSIZ suggested that converting BSIZ into a categorical covariate, by splitting BSIZ into two groups (BSIZ ≤ 1,750 mm^2 and > 1,750 mm^2), provided a better fit than splitting at other values of BSIZ or using a continuous covariate. Therefore, BSIZ was tested as a categorical covariate.

Baseline B-cell counts and diagnosis were confounded, as high B-cell counts were observed in CLL patients. Therefore, diagnosis was used as the primary covariate of interest rather than baseline B-cell count. Models that used B-cell counts as an explanatory covariate were also tested but were shown to be inferior, possibly because B-cell counts were highly variable and dependent on the prior treatment history, being close to or below the detection limit for patients who had prior exposure to B-cell-targeted biologic therapies.

The covariate effects retained in the final model were: weight on clearance and volume parameters; sex on CL_T, CL_{inf}, and central volume (V_1); diagnosis on k_{des}, CL_T, and CL_{inf}; and BSIZ on k_{des}. Age and creatinine clearance did not have a detectable effect on PK parameters. A summary of the parameter estimates of the final covariate model is shown in **Table 3**. While steady-state clearance had moderate (41.5% CV) interindividual variability, time-dependent clearance was

Table 3 Parameter estimates for the final covariate model

Parameter		Estimate	% RSE	95% CI
k_{des} (1/day)	$\exp(\theta_1)$	0.0359	10.8	0.0291–0.0443
$k_{des,DIS}$	$\exp(\theta_{12})$	2.08	12.3	1.63–2.64
$k_{des,BSIZ \le 1,750}$	$\exp(\theta_{15})$	2.65	11.9	2.10–3.35
CL_T (L/day)	$\exp(\theta_2)$	0.231	8.43	0.196–0.272
$CL_{T,SEX}$	$\exp(\theta_9)$	1.49	9.7	1.23–1.80
CL_{inf} (L/day)	$\exp(\theta_3)$	0.0828	3.37	0.0775–0.0884
$CL_{inf,SEX}$	$\exp(\theta_{10})$	1.22	3.6	1.14–1.31
$CL_{inf,WT} = CL_{T,WT}$	θ_7	0.615	14.8	0.437–0.794
$CL_{inf,DIS23} = CL_{T,DIS23}$	$\exp(\theta_{13})$	0.834	3.54	0.778–0.894
$CL_{inf,DIS4} = CL_{T,DIS4}$	$\exp(\theta_{14})$	1.75	17.0	1.25–2.44
V_1 (l)	$\exp(\theta_4)$	2.76	1.38	2.68–2.83
$V_{1,SEX}$	$\exp(\theta_{11})$	1.18	1.83	1.14–1.22
$V_{1,WT}$	θ_8	0.383	12.1	0.293–0.474
V_2 (L)	$\exp(\theta_5)$	1.01	4.47	0.922–1.10
Q (L/day)	$\exp(\theta_6)$	1.29	11.5	1.03–1.62

Parameter		Estimate	% RSE	95% CI	Variability	Shrinkage
ω^2_{kdes}	Ω(1,1)	1.62	7.95	1.37–1.87	CV = 201%	15.4%
ω^2_{CLT}	Ω(2,2)	0.907	11.1	0.71–1.1	CV = 122%	21.6%
ω^2_{CLinf}	Ω(3,3)	0.159	7.12	0.137–0.181	CV = 41.5%	11%
ω^2_{V1}	Ω(4,4)	0.034	9.03	0.028–0.0401	CV = 18.6%	10.8%
ω^2_{V2}	Ω(5,5)	0.361	10.6	0.286–0.436	CV = 65.9%	32.6%
ω^2_{Q}	Ω(6,6)	0.89	17.5	0.585–1.19	CV = 120%	52.2%
ω^2_{EPS}	Ω(7,7)	0.274	10	0.22–0.328	CV = 56.1%	0.1%
σ^2_{prop}	Σ(1,1)	0.0318	4.52	0.029–0.0346	CV = 18.0%	1.8%
σ^2_{add} (μg/ml)^2	Σ(2,2)	0.0271	69.1	0–0.0637	SD = 0.165	

Parameters Q and V_2 were scaled as $(BW/75)^{3/4}$ and $(BW/75)$, respectively. add, additive; BCL, B-cell lymphoma; BSIZ, baseline tumor size; BW, body weight (kg); CI, confidence interval; CL_{inf}, nonspecific time-independent clearance (L/day); $CL_{inf,\ DIS23}$, effect of disease type 2–3 (BCL and DLBCL) on CL_{inf}; $CL_{inf,\ DIS4,}$ effect of disease type 4 (MCL) on CL_{inf}; $CL_{inf,\ WT}$, effect of weight on CL_{inf}; $CL_{inf,\ SEX}$, effect of sex on non CL_{inf}; CL_T, initial value of time-dependent clearance (L/day); $CL_{T,\ DIS23}$, effect of disease type 2–3 (BCL and DLBCL) on CL_T; $CL_{T,\ DIS4,}$ effect of disease type 4 (MCL) on CL_T; $CL_{T,SEX,}$ effect of sex on CL_T; $CL_{T,\ WT}$, effect of weight on CL_T; CV, coefficient of variation (CV = 100*SD%); DLBCL, diffuse large B-cell lymphoma; EPS, epsilon, NONMEM residual error; K_{des}, decay coefficient of time-dependent clearance; $K_{des,\ BSIZ \le 1,750}$, effect of BSIZ ≤ 1,750 mm^2 on K_{des}; $K_{des,\ DIS}$, effect of disease type on K_{des}; MCL, mantle cell lymphoma; prop, proportional; Q, intercompartmental clearance; RSE, relative standard error (RSE = 100·SE/PE, where PE is a parameter estimate); SD, standard deviation; SE, standard error; V_1, central volume; $V_{1,\ SEX}$, effect of sex on V_1; $V_{1,\ WT,}$ effect of weight on V_1; V_2, peripheral volume.

more variable, with interindividual variability of 122% for CL_T and 201% for k_{des}. Inclusion of covariates decreased interindividual variability from 48.1 to 41.5% for CL_{inf}, 24.6 to 18.6% for V_1, 140 to 122% for CL_T, and 233 to 201% for k_{des}.

CL_T was 48.9% (95% CI: 23.1–80.0) higher in males than females. Compared with CLL patients, CL_T and CL_{inf} were lower (–16.6%; 95% CI: –22.2 to –10.6) in individuals with BCL or DLBCL, and were higher in MCL patients (74.6%; 95% CI: 25.1–143.6).

The half-life of CL_T was 19.3 days for CLL patients with high BSIZ (> 1,750 mm^2). K_{des} was 108% (95% CI: 63–164) faster for NHL patients with high BSIZ (half-life of 9.3 days) and 165% (95% CI: 110–235) faster for CLL patients with low BSIZ (≤ 1,750 mm^2; half-life of 7.3 days).

The remaining covariate effects were in the range of 18.1–33.5%. Among them, CL_{inf} and V_1 were slightly higher in males than females (CL_{inf}, 22.4%; 95% CI: 14.0–31.3; V_1, 18.1%; 95% CI: 14.0–22.4), and both positively correlated with weight. CL_T and CL_{inf} were 32.1% (95% CI: 24.0–39.3) lower for 40 kg patients compared with 75 kg patients, and were 33.5% (95% CI: 22.8–45.2) higher for 120 kg patients. Similarly, V_1 was 21.4% (95% CI: 16.8–25.8) lower for 40 kg patients and 19.7% (95% CI: 14.7–24.9) greater for 120 kg patients compared with 75 kg patients.

The goodness-of-fit diagnostic plots of the covariate model did not indicate any model deficiencies (**Supplementary Figure S1**). The dependencies of the random effects on covariates did not show any further trends unaccounted for by the model. Visual predictive check (VPC) simulations indicated good agreement between observed and simulated data for all studies (**Supplementary Figures S2** and **S3**) and covariates (**Supplementary Figure S4**).

Shrinkage was small for all parameters except the parameters of the peripheral compartment. For patients with sparse sampling, there was insufficient information to estimate random effects on V_2 and Q precisely. However, these effects were retained in the model as the IMPMAP estimation method works more efficiently when all fixed effect parameters have an associated random effect.[26,27] Correlation of the random effects was not included in the model, since no correlation was observed for the subset of patients with dense sampling.

Model-based simulations

The effects of covariates on the typical concentration–time courses for patients receiving obinutuzumab 1,000 mg on days 1, 8, and 15 of cycle 1, and day 1 of cycles 2–6 are shown in **Figure 1**. Sex and weight affected the concentration–time course of obinutuzumab (**Figures 1a**,**b**). Serum levels were ~20% lower in men than women (**Figure 1a**). Serum levels among women with the highest body weight were ~60% lower than women with the lowest weight (**Figure 1b**).

Investigation of the impact of diagnosis on the concentration–time course of obinutuzumab (**Figure 1c**) showed that BCL or DLBCL patients had serum levels approximately twice that of MCL patients. CLL patients had serum levels intermediary between BCL or DLBCL patients and MCL patients.

BSIZ also affected serum obinutuzumab levels (**Figure 1d**). Patients with high BSIZ (> 1,750 mm^2) had lower serum levels than individuals with low BSIZ (≤ 1,750 mm^2). These differences were most pronounced during the first 4 months of dosing; from 4 months onwards, obinutuzumab exposure was not affected by BSIZ.

Model-based simulations of the obinutuzumab concentration–time curves (**Figure 2**) showed that steady-state levels were achieved after ~4 months of dosing. The predicted steady-state mean (SD) area under the curve (AUCτ, where τ = 28 days) in BCL or DLBCL patients (12,574 (5,648) μg/ml*h and 12,626 (5,865) μg/ml*h, respectively) was higher than in individuals with CLL (9,943 (4,908) μg/ml*h), while MCL patients had the lowest values (6,038 (3,028) μg/ml*h). Similar trends were observed for minimum (trough) drug concentration (C_{trough}) and maximum drug concentration (C_{max}).

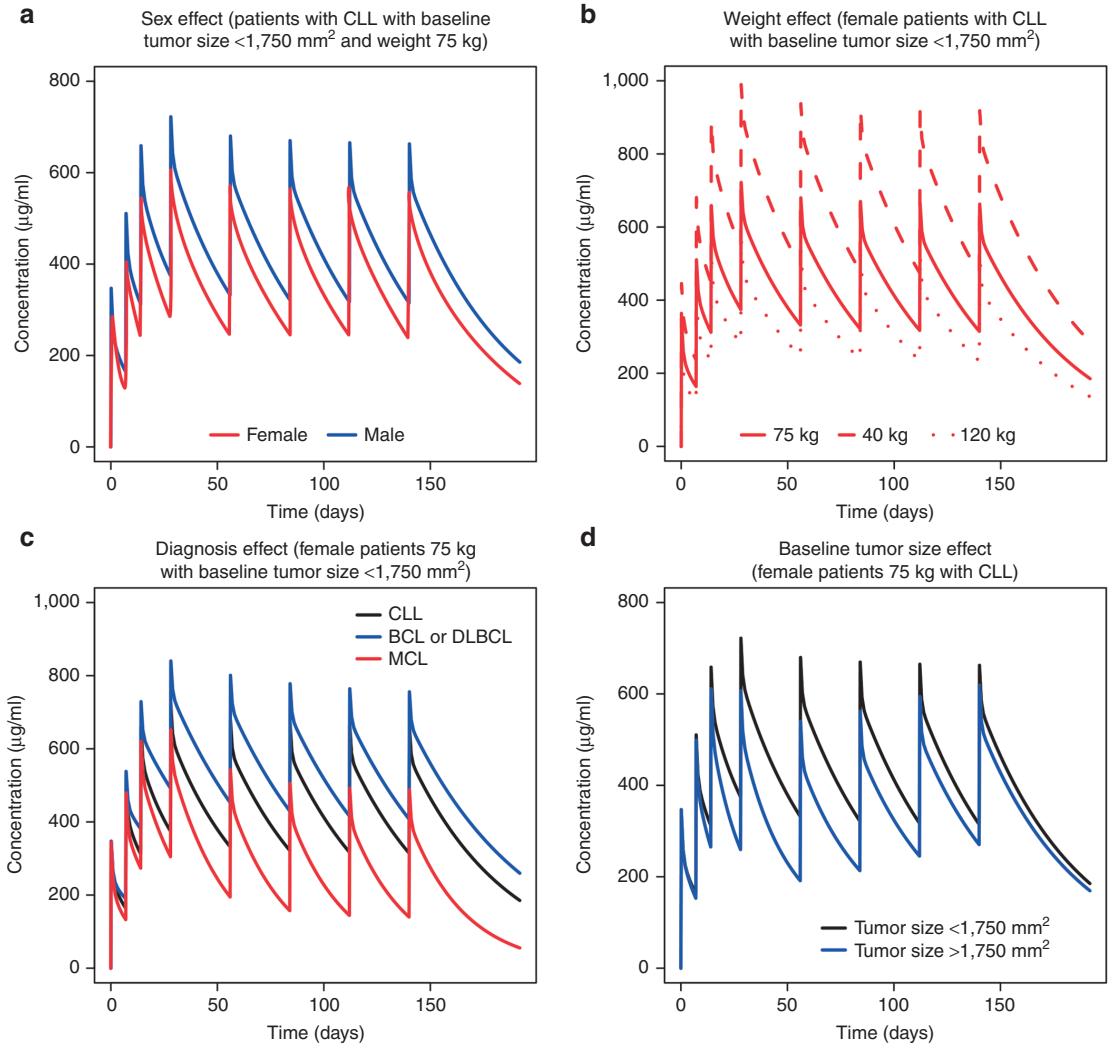

Figure 1 Model-based simulations of a typical obinutuzumab concentration–time course by (**a**) sex, (**b**) weight, (**c**) diagnosis, and (**d**) baseline tumor size. Population predictions for typical patients with specific combinations of covariate values were computed. Concentration–time courses were simulated following 1,000-mg intravenous doses of obinutuzumab on days 1, 8, 15 of cycle 1, and day 1 of cycles 2–6. BCL, B-cell lymphoma; CLL, chronic lymphocytic leukemia; DLBCL, diffuse large B-cell lymphoma; MCL, mantle cell lymphoma.

Impact of obinutuzumab exposure on safety, efficacy, and PD parameters in CLL patients

The relationships between obinutuzumab exposure and response were examined in CLL patients participating in CLL11. Results of the graphical analysis showed no association between the occurence of serious adverse events (SAEs) and serum levels of obinutuzumab: concentration–time profiles for patients who experienced SAEs were similar to those without SAEs. The occurrence and grade of SAEs and infusion-related reactions (IRRs) following the first dose of obinutuzumab were not affected by exposure. Distributions of C_{max} were similar for each grade of IRRs or SAEs following the first dose. For SAEs that occurred following the first dose, occurrence of SAEs did not depend on $C_{max.}$ For SAEs that occurred later on, the occurrence of SAEs was not associated with cumulative AUC or mean exposure (C_{mean}).

The potential association between neutrophil counts and obinutuzumab exposure was also examined. Patients were divided into three groups of similar size based on their exposure to obinutuzumab: C_{mean} < 245 µg/ml (n = 69); 245 µg/ml ≤ C_{mean} ≤ 398 µg/ml (n = 65); C_{mean} > 398 µg/ml (n = 68). Results of the graphical analysis revealed that in all exposure groups, there was no correlation between observed neutropenia and exposure to obinutuzumab; in each exposure group, neutrophil counts were ~5×10^9/L at baseline and declined to 2×10^9/L almost immediately after the start of obinutuzumab administration. When obinutuzumab was no longer in the circulation, neutrophil counts slowly returned to baseline levels. There was also no association between the observed grade of neutropenia and exposure to obinutuzumab; distributions of C_{max} were similar across all grades of neutropenia (0–4), regardless of BSIZ.

There was no association between obinutuzumab exposure (C_{mean} group) and the time course of B-cell counts. At baseline, the mean B-cell count in the total patient population was 31.7×10^9/L; after the start of obinutuzumab administration, B-cell counts decreased to almost zero and remained suppressed throughout the analysis period.

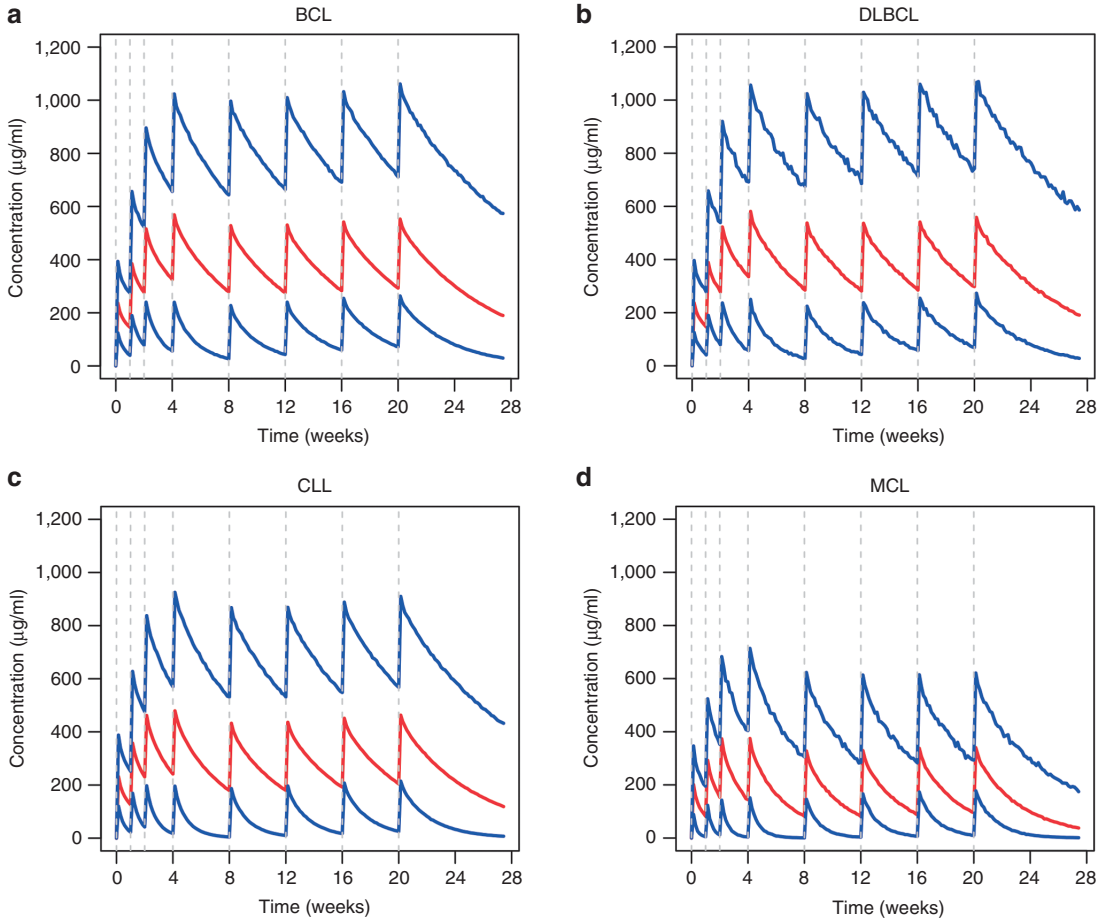

Figure 2 Model-based simulations by diagnosis. Each patient from the analysis data set was used to create 100 simulated patients with the same covariates but different individual random effects. Concentration–time courses were simulated following 1,000 mg intravenous doses of obinutuzumab on days 1, 8, 15 of cycle 1, and day 1 of cycles 2–6. Residual variability was included. Once-a-day sampling was assumed. Medians (red) and 5th and 95th percentiles (blue) of the simulated concentrations are plotted. BCL, B-cell lymphoma; CLL, chronic lymphocytic leukemia; DLBCL, diffuse large B-cell lymphoma; MCL, mantle cell lymphoma.

Percentage change in tumor size from baseline was lower in the low obinutuzumab exposure group than the medium and high exposure groups. When the exposure groups were stratified by BSIZ, the dependency of tumor size change on obinutuzumab exposure remained for patients with a high BSIZ (> 1,750 mm^2), but not for those with a low BSIZ (≤ 1,750 mm^2).

Similarly, for efficacy parameters progression-free survival (PFS) and best overall response (BOR)), higher exposure to obinutuzumab was associated with a more favorable outcome; greater BOR correlated with higher C_{mean} values (**Figure 3a**), which remained when patients were stratified by BSIZ (**Figures 3b**,**c**). Kaplan–Meier survival analysis suggested that a higher exposure to obinutuzumab was also associated with prolonged PFS (**Figure 4a**). However, when the data were stratified by BSIZ, PFS was prolonged only in patients with large BSIZ (> 1,750 mm^2; **Figure 4b**) and not in those with smaller BSIZ (≤ 1,750 mm^2; **Figure 4c**). Overall, insufficient response data were available to support a rigorous PK–PD survival analysis, with very low numbers of patients having stable or progressive disease.

DISCUSSION

This analysis demonstrated that a two-compartment PK model with linear and time-dependent clearance components accurately described the concentration–time course of obinutuzumab in patients with B-cell malignancies, with steady-state PK parameter values typical of monoclonal antibodies.

The PK model is consistent with previous experience, as the PK of antibodies that target B-cell receptors is often time-dependent (e.g., rituximab).[28–31] This is different from the nonlinearity associated with target-mediated drug disposition, and is likely related to depletion of the target or changes in the target expression levels with time, rather than saturation of the target-mediated elimination. Models with target-mediated drug disposition (Michaelis–Menten) elimination terms were also tested, and they were not able to describe the time-dependency of clearance, or significantly improve the model fit. Models relating changes in clearance to the observed depletion of circulating B-cells were also tested, but they were not able to explain the observed dependency of clearance on time. B-cells in circulation are eliminated very rapidly, while the observed time-dependence of clearance

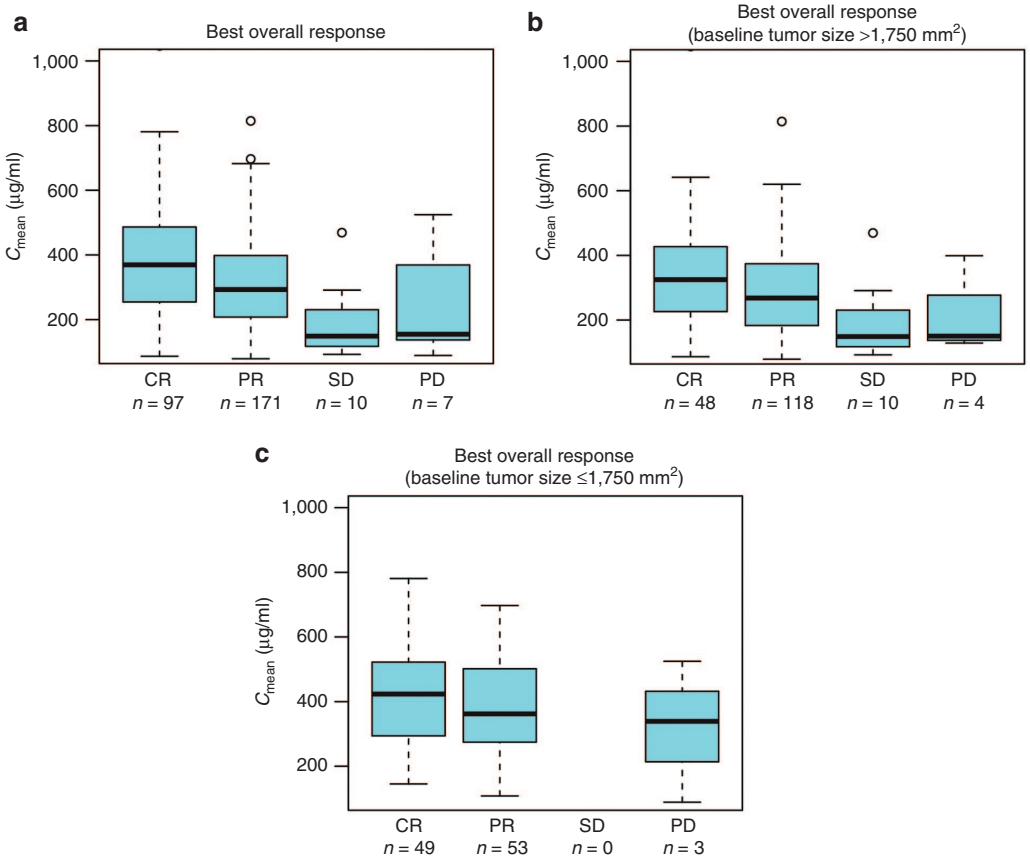

Figure 3 Relationship between best overall response and mean exposure to obinutuzumab. C_{mean} values for obinutuzumab are plotted against BOR using a box and whisker plot. Median values are designated by black lines in the center of the boxes. Boxes indicate the IQR. Whiskers represent the 1.5*IQR. Outliers are marked as circles outside of the whiskers. BOR, best overall response; C_{mean}, mean exposure; CR, complete response; IQR, interquartile range; PD, progressive disease; PR, partial response; SD, stable disease.

has a longer characteristic time scale. Another alternative is to use the latent variable approach, where the latent variable would reflect the disease state and amount of target throughout the body (rather than the target in circulation). In theory, the latent variable model would allow prediction of the increase in clearance following treatment interruptions. However, there were no data available to support estimation of the turnover parameters of latent variable models. After several initial cycles, concentration–time data were well described by a model with time-independent clearance without any evidence of rebound of clearance.

Analysis of covariates showed that clearance (initial and steady-state) and rate of clearance decline were dependent on disease histology (CLL, BCL, DLBCL, or MCL). MCL patients had higher clearance than CLL patients, while individuals with BCL or DLBCL had the lowest clearance. Decline of clearance was faster in NHL patients than CLL patients. These data suggest that tumor type affects obinutuzumab exposure. Higher clearance and slower decrease of clearance in CLL and MCL is consistent with higher levels of target cells (B-cells) in circulation in these diseases compared to BCL and DLBCL, where the majority of malignant cells are located in harder-to-reach tissues. However, clearance in CLL was lower than in MCL, despite higher peripheral B-cell counts in CLL. This is likely due to the significantly higher expression of CD20 receptors on B-cells in MCL patients compared with CLL patients.[32–34]

The decline of clearance was faster for patients with lower BSIZ than for those with higher BSIZ, also consistent with target-mediated drug disposition.

The analysis indicated that the steady-state clearance and volume parameters of obinutuzumab increased with body weight, which is as expected for a monoclonal antibody.[35] Sex had a limited effect on clearance and volume parameters, with men exhibiting higher steady-state clearance and central volume than women. While the reason for this effect is unknown, it could possibly be related to intrinsic differences between males and females in the molecular biology of B-cell malignancies[36] or in FcγRIIIa polymorphisms.[37–39] However, the effects of sex and body weight on the PK of obinutuzumab were not considered to be clinically significant. Additionally, the clearance and volume parameters of obinutuzumab were independent of age and renal function. Overall, these results indicated that no dose adjustments would be necessary for any of these covariates.

Evaluation of exposure–efficacy relationships in CLL patients was complicated by the influence of BSIZ on the PK of obinutuzumab. Patients with a low BSIZ (≤ 1,750 mm²) exhibited higher obinutuzumab exposure during the initial weeks/months of treatment compared with individuals with

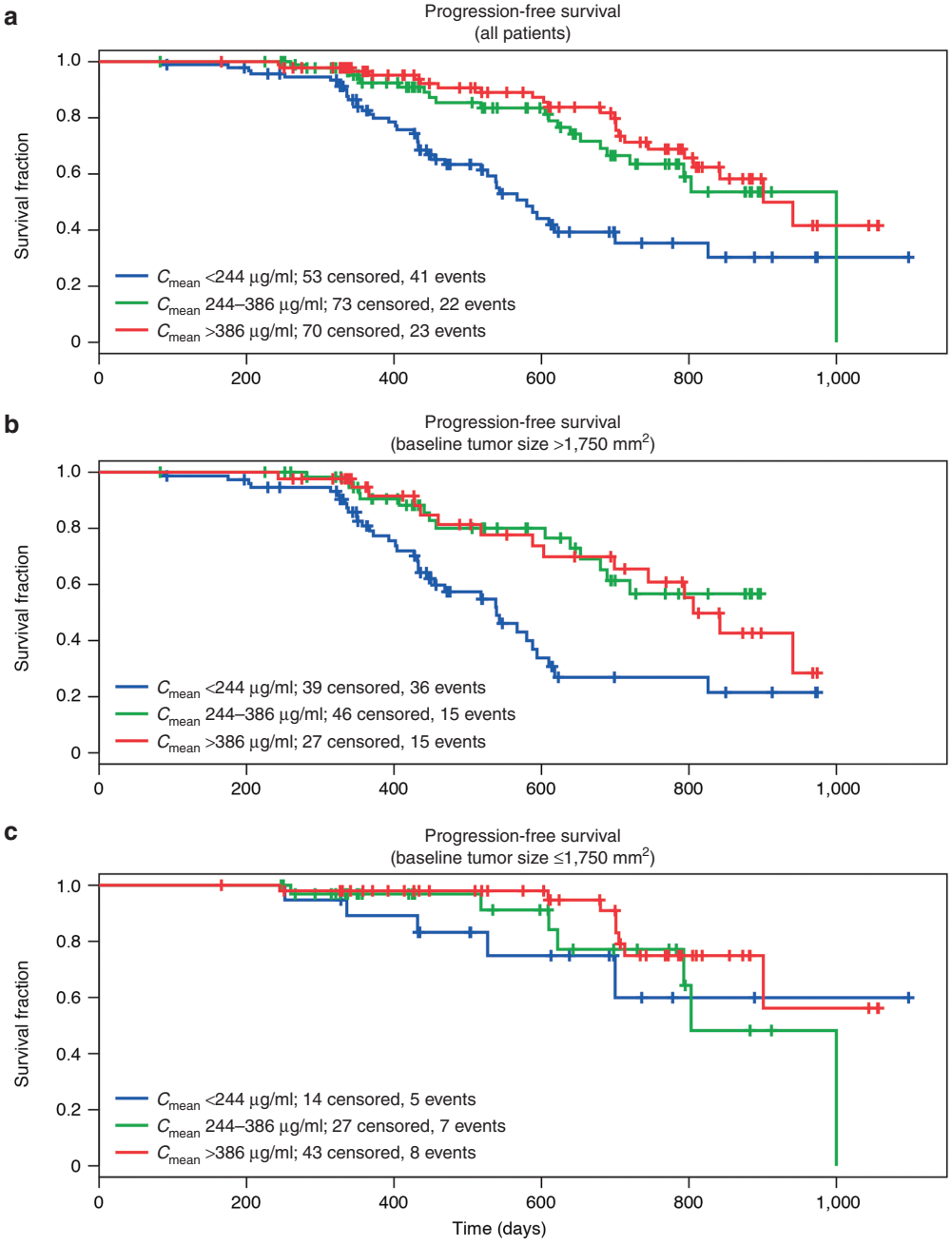

Figure 4 Kaplan–Meier analysis for progression-free survival by obinutuzumab exposure group. Patients in the analysis population were stratified into three groups according to obinutuzumab exposure: C_{mean} < 244 µg/ml; 244 ≤ C_{mean} ≤ 386 µg/ml; C_{mean} > 386 µg/ml. C_{mean}, mean exposure.

a high BSIZ (> 1,750 mm^2). The percentage change in tumor size from baseline was lower in the lowest exposure group than in the higher exposure groups. When patients were stratified by BSIZ, this relationship remained in patients with high BSIZ, but not in those with low BSIZ. There was a trend toward improved BOR for patients with higher exposure to obinutuzumab, which remained after stratification by BSIZ. For PFS, patients who did not have an event had a slightly higher exposure than those who did experience an event, both overall and when stratified by BSIZ. Among patients with events, longer survival appeared to be associated with higher exposure. Kaplan–Meier plots suggested that the observed relationships were mostly due to the lower survival in the lowest exposure group for patients with BSIZ > 1,750 mm^2. Therefore, it was not possible to determine whether adjusting the dose of obinutuzumab would improve efficacy outcomes. Neither the population PK model nor the individual fit identified disease progression as a significant

explanatory covariate for clearance (and hence exposure). After the initial change in clearance, no time dependency of the model parameters was observed, and no influence of disease progression was evident from the diagnostic plots, so dependence of exposure on metrics of survival is unlikely. Further investigation of the impact of exposure on treatment outcomes is warranted.

For all exposure groups, peripheral neutrophil and B-cell counts decreased from baseline after the start of obinutuzumab administration and remained low for the duration of the study. The maximum effect was already reached in the lowest exposure group; no further decline in B-cell or neutrophil counts or neutropenia grade was observed in the higher exposure groups. There was no relationship between obinutuzumab concentrations and the occurrence of SAEs. No association was found between predicted C_{max} of obinutuzumab following the first dose and occurrence of SAEs or IRRs following the first dose. There was also no correlation between obinutuzumab exposure (cumulative AUC and C_{mean}) and occurrence of later SAEs.

In conclusion, a PK model with linear and time-dependent clearance components developed in this analysis accurately estimated the concentration–time course of obinutuzumab in NHL and CLL patients. The strong clinical response of CLL patients when treated with obinutuzumab supports the dose and regimen administered (1,000 mg in cycle 1 (days 1, 8, and 15) and 1,000 mg in cycles 2–6 on day 1). It was found that clearance of obinutuzumab was mainly affected by diagnosis and BSIZ. While the results of exposure–response analysis of safety parameters for CLL patients demonstrated no association between safety and exposure to obinutuzumab, the suggestion of improved efficacy with increased exposure in patients with high tumor burden requires further investigation.

METHODS

Patients and study designs

The PK model was developed using clinical data from patients with CD20+ NHL or CLL participating in GAUGUIN (BO20999; NCT00517530), GAUDI (BO21000; NCT00825149), GAUSS (BO21003; NCT00576758), and CLL11 (BO21004; NCT01010061). In these studies, obinutuzumab was administered at a dose of 200–2,000 mg by intravenous (IV) infusion (maximum rate of 400 mg/h). Details are shown in **Table 1**. All studies were conducted in accordance with the principles of the Declaration of Helsinki and the International Conference on Harmonization Guidelines for Good Clinical Practice. Each study protocol was approved by the ethics committee at participating study centers.

Serum sampling and bioanalytical methods

Table 1 shows details of the serum sampling schedule for each study. Obinutuzumab concentration in serum samples was determined using an established and validated sandwich enzyme-linked immunosorbant assay.[19,20,40] The lower limit of quantification was 4.05 ng/ml. Concentrations were below this limit in 74 postdose observations (0.6% of samples); these observations were excluded from the analysis.

Base PK model development

Analysis of the population PK data was conducted using nonlinear mixed-effects modeling with NONMEM software version 7.2.0 (Icon Development Solutions, Ellicott City, MD).[26] The Monte Carlo importance sampling expectation–maximization assisted by mode *a posteriori* estimation (IMPMAP) method was used. The IMPMAP method is faster than the first-order conditional estimation with interaction method, while providing the same level of information for target-mediated drug disposition -type models in monoclonal antibodies.[27] The PK of monoclonal antibodies are usually described by a two-compartment model, either linear or with target-mediated disposition. B-cell-targeting monoclonal antibodies such as rituximab have also been shown to exhibit time-dependent clearance, a possible reflection of treatment-related decreases in target B-cell counts over time. Therefore, the initial two-compartment model was tested using a linear elimination, a parallel linear and Michaelis–Menten elimination, or a time-dependent clearance. In the time-dependent clearance model, clearance (CL) was the sum of the time-dependent (CL_t) and time-independent (CL_{inf}) terms ($CL = CL_t + CL_{inf}$). Time-dependent clearance decreased with time as $CL_t = CL_T \exp(-k_{des} TIME)$, where CL_T is the initial value of time-dependent clearance and k_{des} is the decay coefficient of time-dependent clearance.

As a starting point, log-normally distributed interindividual random effects were introduced for all structural parameters and the residual error for observations was described by the combined additive and multiplicative error model. Model refinement was data-driven and based on goodness-of-fit indicators. During modeling, correlation of the random effects was observed for patients with dense sampling; therefore, it was not included in the model. Allometric scaling of body weight with fixed power coefficients (0.75 and 1 for all clearance and volume parameters, respectively) was introduced during base model development.

Covariate model development

A full covariate modeling approach emphasizing parameter estimation was used to develop the covariate model. Multiple covariates were simultaneously added to model parameters, including sex, body weight, age, BSIZ, baseline B-cell count, and diagnosis (CLL, BCL, DLBCL, or MCL). These covariates were chosen based on mechanistic plausibility, exploratory analysis, and scientific interest. The covariate model was refined based on point estimates, CIs, and diagnostic plots rather than on the OFV. The number of estimated parameters was reduced by eliminating small and well-estimated effects (where CIs included null values) and by grouping together categorical covariates with similar effects. The effects of categorical covariates were tested as binary covariates; the effects of continuous covariates were modeled using a normalized power model. Other covariates (normalized creatinine clearance, presence of antidrug antibodies) were evaluated by diagnostic plots. The NONMEM code for the final model is shown in **Supplementary Table S1**.

Model evaluation

All models were evaluated graphically using goodness-of-fit plots. Estimates of precision (asymptotic standard of error; 95% CIs) were calculated for each model parameter. The degree of regression to the mean was evaluated by computing the shrinkage for all random effects.[41] Various visual predictive checks, including VPC, standardized VPC, prediction-corrected VPC, and normalized prediction distribution error,[42–45] were performed for the base and final covariate models, overall for all data and stratified by study, diagnosis, weight, or sex.

Model-based simulations

The final PK model was used to simulate the expected obinutuzumab concentration–time course for the dosing regimen used in CLL11 (1,000 mg IV every 4 weeks for 20 weeks with additional 1,000-mg IV doses on days 8 and 15 of cycle 1). The simulations were used to (i) evaluate the effects of covariates, (ii) determine the spread of concentrations and approach to steady-state, and (iii) compute steady-state PK parameters, such as AUC_{τ}, C_{max}, and C_{trough}.

Graphical analysis of exposure–safety and exposure–efficacy relationships for CLL patients (CLL11 study)

The exposure–safety analysis examined the relationship between obinutuzumab exposure and SAEs, IRRs, and the time–course of neutrophil counts. The exposure–efficacy analysis evaluated relationships between obinutuzumab exposure and PD parameters (B-cell counts, tumor size) and efficacy outcomes (BOR, PFS). The evaluated exposure metrics depended on the response end-point and included maximum concentration following the first dose (C_{max}), cumulative AUC from the first dose until the event (AUC_{cum}), or mean exposure (C_{mean}) defined as AUC_{cum} divided by time elapsed from the first dose.

A total of 49 (15.9%) of the CLL11 patients whose data were used for the graphical exposure–response analysis dropped out from the study (for reasons not related to disease progression); these patients were included as censored observations.

Acknowledgments. Support for third-party writing assistance for this manuscript was provided by F. Hoffmann-La Roche Ltd.

Author Contributions. V.B. and N.F. collected data. E.G., L.G., and N.F. analyzed data. E.G., L.G., D.C., and N.F. interpreted the data. E.G., L.G., C.J., N.F., D. C., and V.B. wrote the manuscript. E.G., L.G., C.J., N.F., D. C., and V.B. approved the final version.

Conflict of Interest. E.G. and L.G. were consultants for Hoffmann-La Roche. C.J., D.C., and N.F. are employees of Hoffmann-La Roche.

Study Highlights

WHAT IS THE CURRENT KNOWLEDGE ON THE TOPIC?

✓ Treatment regimens involving obinutuzumab exhibited enhanced antitumor activity compared with rituximab in clinical trials of NHL and CLL. However, the PK properties and the exposure–response relationships of obinutuzumab still need to be adequately described.

WHAT QUESTION DID THIS STUDY ADDRESS?

✓ This analysis characterized the PK properties of obinutuzumab in patients with CLL and NHL and exposure–response relationships in those with CLL.

WHAT THIS STUDY ADDS TO OUR KNOWLEDGE

✓ The concentration–time course of obinutuzumab was described by a two-compartment PK model with parallel linear and time-dependent clearance. PK parameters were mainly affected by diagnosis and BSIZ. In patients with CLL, exposure was not associated with safety. Exposure positively correlated with efficacy, but this observation was confounded by the association of high exposure with low BSIZ.

HOW THIS MIGHT CHANGE CLINICAL PHARMACOLOGY AND THERAPEUTICS

✓ This analysis confirmed that the 1,000 mg fixed dose provides an appropriate response in the NHL population. However, it may be of interest to investigate whether increasing the exposure improves efficacy in patients with a high baseline tumor burden.

1. Coiffier, B. *et al.* CHOP chemotherapy plus rituximab compared with CHOP alone in elderly patients with diffuse large-B-cell lymphoma. *N. Engl. J. Med.* **346**, 235–242 (2002).
2. Coiffier, B. *et al.* Long-term outcome of patients in the LNH-98.5 trial, the first randomized study comparing rituximab-CHOP to standard CHOP chemotherapy in DLBCL patients: a study by the Groupe d'Etudes des Lymphomes de l'Adulte. *Blood* **116**, 2040–2045 (2010).
3. Pfreundschuh, M. *et al.*; MabThera International Trial Group. CHOP-like chemotherapy plus rituximab versus CHOP-like chemotherapy alone in young patients with good-prognosis diffuse large-B-cell lymphoma: a randomised controlled trial by the MabThera International Trial (MInT) Group. *Lancet. Oncol.* **7**, 379–391 (2006).
4. Marcus, R. *et al.* CVP chemotherapy plus rituximab compared with CVP as first-line treatment for advanced follicular lymphoma. *Blood* **105**, 1417–1423 (2005).
5. Forstpointner, R. *et al.*; German Low-Grade Lymphoma Study Group. The addition of rituximab to a combination of fludarabine, cyclophosphamide, mitoxantrone (FCM) significantly increases the response rate and prolongs survival as compared with FCM alone in patients with relapsed and refractory follicular and mantle cell lymphomas: results of a prospective randomized study of the German Low-Grade Lymphoma Study Group. *Blood* **104**, 3064–3071 (2004).
6. Hiddemann, W. *et al.* Frontline therapy with rituximab added to the combination of cyclophosphamide, doxorubicin, vincristine, and prednisone (CHOP) significantly improves

the outcome for patients with advanced-stage follicular lymphoma compared with therapy with CHOP alone: results of a prospective randomized study of the German Low-Grade Lymphoma Study Group. *Blood* **106**, 3725–3732 (2005).
7. Schulz, H. *et al.* Immunochemotherapy with rituximab and overall survival in patients with indolent or mantle cell lymphoma: a systematic review and meta-analysis. *J. Natl. Cancer Inst.* **99**, 706–714 (2007).
8. Herold, M. *et al.*; East German Study Group Hematology and Oncology Study. Rituximab added to first-line mitoxantrone, chlorambucil, and prednisolone chemotherapy followed by interferon maintenance prolongs survival in patients with advanced follicular lymphoma: an East German Study Group Hematology and Oncology Study. *J. Clin. Oncol.* **25**, 1986–1992 (2007).
9. Salles, G. *et al.* Rituximab maintenance for 2 years in patients with high tumour burden follicular lymphoma responding to rituximab plus chemotherapy (PRIMA): a phase 3, randomised controlled trial. *Lancet* **377**, 42–51 (2011).
10. van Oers, M.H. *et al.* Rituximab maintenance treatment of relapsed/resistant follicular non-Hodgkin's lymphoma: long-term outcome of the EORTC 20981 phase III randomized intergroup study. *J. Clin. Oncol.* **28**, 2853–2858 (2010).
11. Cheson, B.D. *et al.*; International Working Group for Diagnosis, Standardization of Response Criteria, Treatment Outcomes, and Reporting Standards for Therapeutic Trials in Acute Myeloid Leukemia. Revised recommendations of the International Working Group for Diagnosis, Standardization of Response Criteria, Treatment Outcomes, and Reporting Standards for Therapeutic Trials in Acute Myeloid Leukemia. *J. Clin. Oncol.* **21**, 4642–4649 (2003).
12. Hagemeister, F. Rituximab for the treatment of non-Hodgkin's lymphoma and chronic lymphocytic leukaemia. *Drugs* **70**, 261–272 (2010).
13. Keating, G.M. Rituximab: a review of its use in chronic lymphocytic leukaemia, low-grade or follicular lymphoma and diffuse large B-cell lymphoma. *Drugs* **70**, 1445–1476 (2010).
14. Mössner, E. *et al.* Increasing the efficacy of CD20 antibody therapy through the engineering of a new type II anti-CD20 antibody with enhanced direct and immune effector cell-mediated B-cell cytotoxicity. *Blood* **115**, 4393–4402 (2010).
15. Niederfellner, G. *et al.* Epitope characterization and crystal structure of GA101 provide insights into the molecular basis for type I/II distinction of CD20 antibodies. *Blood* **118**, 358–367 (2011).
16. Glennie, M.J., French, R.R., Cragg, M.S. & Taylor, R.P. Mechanisms of killing by anti-CD20 monoclonal antibodies. *Mol. Immunol.* **44**, 3823–3837 (2007).
17. Morschhauser, F. *et al.* Humanized anti-CD20 antibody, veltuzumab, in refractory/recurrent non-Hodgkin's lymphoma: phase I/II results. *J. Clin. Oncol.* **27**, 3346–3353 (2009).
18. Morschhauser, F. *et al.* Results of a phase I/II study of ocrelizumab, a fully humanized anti-CD20 mAb, in patients with relapsed/refractory follicular lymphoma. *Ann. Oncol.* **21**, 1870–1876 (2010).
19. Salles, G. *et al.* Phase 1 study results of the type II glycoengineered humanized anti-CD20 monoclonal antibody obinutuzumab (GA101) in B-cell lymphoma patients. *Blood* **119**, 5126–5132 (2012).
20. Sehn, L.H. *et al.* A phase 1 study of obinutuzumab induction followed by 2 years of maintenance in patients with relapsed CD20-positive B-cell malignancies. *Blood* **119**, 5118–5125 (2012).
21. Sehn, L.H. *et al.* Randomized phase II trial comparing GA101 (obinutuzumab) with rituximab in patients with relapsed CD20+ indolent B-cell non-Hodgkin lymphoma: preliminary analysis of GAUSS study. *Blood* **118**, Abstract 269 (2011).
22. Morschhauser, F.A. *et al.* Obinutuzumab (GA101) monotherapy in relapsed/refractory diffuse large b-cell lymphoma or mantle-cell lymphoma: results from the phase II GAUGUIN study. *J. Clin. Oncol.* **31**, 2912–2919 (2013).
23. Salles, G.A. *et al.* Obinutuzumab (GA101) in patients with relapsed/refractory indolent non-Hodgkin lymphoma: results from the phase II GAUGUIN study. *J. Clin. Oncol.* **31**, 2920–2926 (2013).
24. Radford, J. *et al.* Obinutuzumab (GA101) plus CHOP or FC in relapsed/refractory follicular lymphoma: results of the GAUDI study (BO21000). *Blood* **122**, 1137–1143 (2013).
25. Goede, V. *et al.* Obinutuzumab plus chlorambucil in patients with CLL and coexisting conditions. *N. Engl. J. Med.* **370**, 1101–1110 (2014).
26. Beal, S.L., Sheiner, L.B., Boeckmann, A.J. & Bauer, R.J. *NONMEM Users Guides. 1989–2011* (Icon Development Solutions, Ellicott City, Maryland, USA, 2011).
27. Gibiansky, L., Gibiansky, E. & Bauer, R. Comparison of Nonmem 7.2 estimation methods and parallel processing efficiency on a target-mediated drug disposition model. *J. Pharmacokinet. Pharmacodyn.* **39**, 17–35 (2012).
28. Levi, M. *et al.* Characterization of the time-varying clearance of rituximab in nonhodgkin's lymphoma patients using a population pharmacokinetic analysis. Abstract from The American Conference on Pharmacometrics, 2008. <http://tucson2008.go-acop.org/pdfs/Levi.pdf>. Accessed 2 July 2014.
29. Yin, A. *et al.* Population pharmacokinetics (PK) and association of PK and clinical outcomes of rituximab in patients with non-Hodgkin's lymphoma. *J. Clin. Oncol.* **28**, Abstract e13108 (2010).
30. Li, J. *et al.* Population pharmacokinetics of rituximab in patients with chronic lymphocytic leukemia. *J. Clin. Pharmacol.* **52**, 1918–1926 (2012).
31. Australian Government Department of Health and Ageing: Therapeutic Drugs Administration. Australian Public Assessment Report for Rituximab, December 2011. <http://www.tga.gov.au/pdf/auspar/auspar-mabthera-111215.pdf>. Accessed 2 July 2014.
32. Ginaldi, L., De Martinis, M., Matutes, E., Farahat, N., Morilla, R. & Catovsky, D. Levels of expression of CD19 and CD20 in chronic B cell leukaemias. *J. Clin. Pathol.* **51**, 364–369 (1998).
33. Suková, V., Klabusay, M., Coupek, P., Brychtová, Y., Doubek, M. & Mayer, J. Density expression of the CD20 antigen on population of tumor cells in patients with chronic B-lymphocyte lymphoproliferative diseases. *Cas. Lek. Cesk.* **145**, 712–6; discussion 716 (2006).
34. Prevodnik, V.K., Lavrenčak, J., Horvat, M. & Novakovič, B.J. The predictive significance of CD20 expression in B-cell lymphomas. *Diagn. Pathol.* **6**, 33 (2011).
35. Ling, J., Zhou, H., Jiao, Q. & Davis, H.M. Interspecies scaling of therapeutic monoclonal antibodies: initial look. *J. Clin. Pharmacol.* **49**, 1382–1402 (2009).
36. Molica, S. Sex differences in incidence and outcome of chronic lymphocytic leukemia patients. *Leuk. Lymphoma* **47**, 1477–1480 (2006).
37. Kastbom, A. *et al.* Influence of FCGR3A genotype on the therapeutic response to rituximab in rheumatoid arthritis: an observational cohort study. *BMJ Open* **2**, (2012).
38. Kastbom, A., Ahmadi, A., Söderkvist, P. & Skogh, T. The 158V polymorphism of Fc gamma receptor type IIIA in early rheumatoid arthritis: increased susceptibility and severity in male patients (the Swedish TIRA project). *Rheumatology (Oxford).* **44**, 1294–1298 (2005).
39. Mellor, J.D., Brown, M.P., Irving, H.R., Zalcberg, J.R. & Dobrovic, A. A critical review of the role of Fc gamma receptor polymorphisms in the response to monoclonal antibodies in cancer. *J. Hematol. Oncol.* **6**, 1 (2013).
40. Ogura, M. *et al.* Phase I study of obinutuzumab (GA101) in Japanese patients with relapsed or refractory B-cell non-Hodgkin lymphoma. *Cancer Sci.* **104**, 105–110 (2013).
41. Karlsson, M.O. & Savic, R.M. Diagnosing model diagnostics. *Clin. Pharmacol. Ther.* **82**, 17–20 (2007).
42. Yano, Y., Beal, S.L. & Sheiner, L.B. Evaluating pharmacokinetic/pharmacodynamic models using the posterior predictive check. *J. Pharmacokinet. Pharmacodyn.* **28**, 171–192 (2001).
43. Wang, D.D. & Zhang, S. Standardized visual predictive check versus visual predictive check for model evaluation. *J. Clin. Pharmacol.* **52**, 39–54 (2012).
44. Bergstrand, M., Hooker, A.C., Wallin, J.E. & Karlsson, M.O. Prediction-corrected visual predictive checks for diagnosing nonlinear mixed-effects models. *AAPS J.* **13**, 143–151 (2011).
45. Mentré, F. & Escolano, S. Prediction discrepancies for the evaluation of nonlinear mixed-effects models. *J. Pharmacokinet. Pharmacodyn.* **33**, 345–367 (2006).

Supplementary information accompanies this paper on the *CPT: Pharmacometrics & Systems Pharmacology* website (http://www.nature.com/psp)